The thermal stability of the *Fusarium solani pisi* cutinase as a function of pH

Steffen B. Petersen,[*] Peter Fojan, Evamaria I. Petersen, and Maria Teresa Neves Petersen

Institute of Life Science, Sohngaardsholmsvej 49, Dk-9000 Aalborg, Denmark

We have investigated the thermal stability of the *Fusarium solani pisi* cutinase as a function of pH, in the range from pH 2–12. Its highest enzymatic activity coincides with the pH-range at which it displays its highest thermal stability. The unfolding of the enzyme as a function of pH was investigated by microcalorimetry. The ratio between the calorimetric enthalpy ($\triangle H_{cal}$) and the van't Hoff enthalpy ($\triangle H_v$) obtained, is far from unity, indicating that cutinase does not exhibit a simple two state unfolding behaviour. The role of pH on the electrostatic contribution to the thermal stability was assessed using TITRA. We propose a molecular interpretation for the pH-variation in enzymatic activity.

INTRODUCTION

Cutinase is a lipolytic enzyme, present in many different organisms, from prokaryotes to eukaryotes. Lipases are widely found in fungi. When testing for lipase activity in the alkaline region, from pH 7 and above, only 25% of the lipase producing fungi show activity in that range [1]. It appears as if the genus *Fusarium* produces exceptionally high activity lipases. In addition to lipase activity, the lipase produced by these fungi showed some hydrolytic activity towards cutin and suberin. The cutinase isolated from the fungus *Fusarium solani pisi*, is assumed to be involved in the first steps of fungal attack on plants [2]. A cutinase found in the fungus *Aspergillus oryzae*, used in the soy bean fermentation industry, has been isolated and appears to be responsible for the flavor formation in soy bean oil [3]. Studies on structure function relationships were carried out using *F. solani pisi* cutinase, produced in *E. coli*, as a model enzyme.

The properties of a protein will be influenced by the local physical chemical environment that it is immersed in. Thus pH, salt, solvent, and temperature are important factors. In particular pH will change the thermostability of a protein and at extreme basic or acidic values, the protein may become significantly destabilized or even denature. Other proteins may be latently unstable even within their active pH-range, such a case has recently been reported [4]. Differential Scanning Calorimetry (DSC) allows for a direct study of the influence of pH on the thermal stability of proteins. Thus we may investigate the T_m's (midpoint of transition) dependence on pH at a given scanrate, and relate the obtained data to changes in 3D structure and to the pH activity profile of the protein. In the present study the thermal stability of the lipolytic enzyme cutinase from *F. solani pisi* as a function of pH was investigated. We have correlated our observations from microcalorimetry, with the pH activity profile and the electrostatic potential distribution on the molecular surface at different pH values, using the available high resolution X-ray structural data for the enzyme [5].

At the temperature T_m where the protein is loosing (part of) its 3D structure, the excess heat capacity increases sharply. This heat capacity is directly related to the protein unfolding process. It is likely that the underlying process is only representing the first (rapid) unfolding step, thus more (slower) processes may take place at temperatures above T_m. This first fast step of the unfolding process may result in a molten globule state of the protein. The stability of such an intermediate state in the unfolding process may be very short lived and thus may not be experimentally accessible for a variety of proteins. During thermal denaturation irreversible processes may also take place (*e.g.*, protein self aggregation, or deamidation found at basic pH values), preventing the protein from refolding. Differential scanning calorimetry (DSC) allows accurate investigation of the thermal stability of proteins as well as other biological macromolecules and aggregates. The methodology allows for the utilization of very different temperature scanning rates. In the past few years a variety of methods and theoretical models have been established to characterise the different unfolding behavior of proteins [6, 7]. Microcalorimetry is a very powerful method to probe the thermal stability, but the sensitivity of the method is still restricted by the protein concentration. More sensitive methods to probe for the thermal stability of a protein may be fluorescence spectroscopy or CD. These methods are capable of measuring the midpoint of transition at protein concentrations inaccessible for DSC. Since protein aggregation is strongly concentration-dependent, these methods are well suited alternatives to improve the quality of the obtained data.

Forces that contribute to the stability of proteins are of various nature and their size and contribution to the protein stability, is a widely discussed topic. These also include elec-

trostatic interactions. It has been found that unfavourable charge distribution on the surface of proteins are capable of destabilising the protein [8]. The electrostatic interactions, on the other hand, are able to contribute positively to the protein stabilisation as well, by forming ionic interactions (salt bridges) between residues carrying opposite charges. When investigating the thermal stability of a protein with respect to pH, the electrostatic interactions in the protein are probed for, since their strength and sign depends on pH. Protein electrostatic calculations have been applied in the discussion about the intermolecular forces determining the stability of proteins. The stability of proteins depends on noncovalent electrostatic and hydrophobic interaction energies of the order of 20–40 kJmol^{-1} [9]. The electrostatic interactions of proteins facilitate long ranged inter- and intramolecular forces. Being the strongest long range force known they are a major determinant of properties such as function and stability of proteins and other biomolecules. The study of the role of electrostatics in protein function, stability and folding/unfolding, involves the study of pH effects in molecular systems. The key factor influencing the activity of many enzymes is pH, because enzymes require that the catalytic residues have the appropriate protonation state in their active pH-range. Usually, proteins become unstable at extreme pH values, not only because of acid- and base-catalysed reactions but also because of changes in the formal charge state of the titratable groups. It is clear that a successful structure-based model for the prediction of the pH-dependent phenomena would contribute significantly to our understanding of enzyme mechanisms, protein stability, and molecular recognition.

The direct result of a pH change is a modification in the equilibrium concentrations of the protonated and deprotonated forms of titratable sites, whose most pronounced consequence is a corresponding change in the balance of charges. These charges will induce a potential distribution on the protein surface that will be pH-dependent. Thus, the consideration of pH effects on proteins is to a great extent an electrostatic problem.

MATERIALS AND METHODS

DSC

The experiments were done using a MicroCal VP-DSC microcalorimeter with a cell volume of 0.52 ml, under a constant pressure of 30 psi, in order to avoid the formation of gas bubbles during the experiment. The instrument was interfaced to a PC equipped with a data translation board for instrument control and automatic data collection. The enzyme concentrations used in the experiments were 0.7 mgml^{-1}. Samples were degassed for at least 20 minutes prior to the experiments, using a membrane vacuum pump. Correction of instrument response time was done automatically by the software. To provide maximum reproducibility of data, taking the thermal history of the instrument into account, scans were performed with the same start temperature and also ending temperature. The excess heat capacity functions were obtained by baseline

subtraction and concentration normalization. Data processing was done with the Microsoft Windows-based software package Origin^{TM}, provided by MicroCal^{TM}. For the analysis a model has been established, taking into account that no intermediate state during the unfolding reaction has been found. Under this assumption we established the following model, that the native protein (N) unfolds into an unfolded state (U), and reacts further to a denatured state D. (1)

$$\text{N} \underset{k2}{\overset{k1}{\rightleftarrows}} \text{U} \xrightarrow{k3} \text{D}. \tag{1}$$
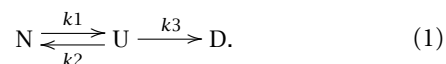
The mathematical formulas used for the data processing are derived from the thermodynamic equations (2), (3), and (4) [6], excluding $\triangle C_p$ effects:

$$C_p(T) = \frac{K(T)^* \triangle H_{cal}^* \triangle H_{vH}}{(1 + K(T))^2 * R * T^2}, \tag{2}$$

$$K(T) = \exp\left\{ \frac{-\triangle H_{vH}}{RT}\left(1 - \left(\frac{T}{T_m} \right) \right) \right\}, \tag{3}$$

$$\left(\frac{v}{T_m^2} \right) = \left(\frac{A_0 E_a}{R} \right) \exp^{-E_a/(RT_m)}, \tag{4}$$

T_m is the midpoint of the calorimetric transition

E_a is the activation energy for the protein unfolding

$C_p(T)$ is the excess heat capacity recorded by the instrument

A_0 is the Arrhenius frequency factor

v is the scanrate

R is the gas constant

$\triangle H_{cal}$ is the calorimetric enthalpy

$\triangle H_{vH}$ is the vant Hoff enthalpy

The calorimetric and vant Hoff enthalpies were calculated from the thermograms by a nonlinear least squares fit to equation (4).

EXPRESSION OF THE CUTINASE GENE IN *E. COLI* AND PURIFICATION OF THE PROTEIN

For the expression of the *F. solani* cutinase gene in *E. coli* BL21(DE3) a T7 promoter based expression system was used (pFCEX1). The cells were grown at 25°C in 1 l of Luria Broth (LB) [10] containing ampicillin (100 μg/ml). 250 ml of medium was used in 1 l of shikane shaking flasks at 400 rpm. Induction of the cultures were carried out at OD$_{600}$ 1.5 for about 6 hours with 0.1 mM isopropyl-b-D-thiogalactopyranoside (IPTG).

Since the cutinase gene (*cut*) is cloned behind the signal peptide for the alkaline phosphatase (*phoA*) the gene product is directed to the periplasm of *E. coli*. The preparation of the periplasmic fraction is performed by an osmotic shock using a TES buffer (50 mM Tris, 10 mM EDTA, 20% sucrose, pH 7.5 adjusted with HCl). Afterwards the cells are washed with pure water. The supernatants of the TES and the water fractions contain cutinase, at about 80%–90% purity. For further purification both fractions

are applied to a high-resolution strong cation-exchange column (SP Sepharose Fast Flow; Pharmacia LKB). Following this protocol, which is a modification of the protocol published in Lauwereys M, 1990 [11] we could achieve an estimated 98%–100% purification of the cutinase of both fractions.

pK VALUES OF BUFFERS, TEMPERATURE SENSITIVITY

For the DSC experiment the choice of buffer is essential, because of the heating of the solution. The initial pH adjustment is done at 25°C. The drift of pH should be as low as possible, to ensure a constant pH environment. The buffer ionization enthalpies (ranked by pK_a, $\triangle pK_a / \triangle T$ values) are: (sodium phosphate 2.15; +0.0044) (acetate 4.76, −0.0002) (citrate 6.40, 0.0000) (tris 8.06, −0.0280).

PROTEIN ELECTROSTATICS

Monitoring the electrostatic changes on the protein surface, two programs were used to take all considerations affecting the protein stability into account. The program acc-run was used to calculate the solvent accessible area of each residue of cutinase. The program TITRA [12] was then used to predict the partial charges of the titratable sites on cutinase, using the two accessibility files computed by acc-run as input files [13].

The program TITRA is a protein titration program implementing the modified Tanford-Kirkwood sphere model for site-site interactions [14] and the Tanford-Roxby iterative mean field approximation [15] for calculation of the average protonation state of the titratable sites [13].

The calculated charges, by using TITRA, carried by the titratable residues of the protein are then supplied to Del-Phi [16] in order to calculate the three-dimensional potential grid for the protein at a particular pH value. Based on these grid data from DelPhi, the electrostatic properties were mapped on the molecular surface of cutinase using the program GRASP (Figure 6). This procedure has been done to be able to visualize the location of the charges on the surface of the protein. The program Titra is capable of calculating the pK_a values of titratable amino acids very precisely as seen for ubiquitin where the pKa values have been determined experimentally [17].

RESULTS

The thermal unfolding of cutinase was investigated as a function of pH in different buffers. In the pH range from 2 to 4 NaH_2PO_4, was used in the range of 4 to 5.5 NaOAc buffer, in the range of 6 to 7.5 Sodium citrate buffer, and above 7.5 TRIS buffer was used at a buffer concentration of 20 mM for the calorimetric investigations. The pH of the buffer was adjusted with NaOH. Except for the TRIS buffer, having the highest ionization enthalpy, buffers displaying a low buffer ionization enthalpy over the temperature range applied for the calorimeter scans have been selected and therefore pro-

TABLE 1: pH dependence profile of native Cutinase. Native Cutinase shows refolding up to pH 5.5. Beyond pH 6.0 no refolding is seen in DSC experiments due to irreversible self aggregation. $T_{1/2}$ denotes the peak halfwidth, ΔH_{cal} is the calorimetric enthalpy and ΔH_{vh} is the vant Hoff enthalpy. The enthalpy values are given in kcal/mol.

pH	T_m	$T_{1/2}$	ΔH_{cal}	$\Delta H_{cal} / \Delta H_v$
2.75	30.03	5.59933	7.30	0.0619
3	34.98	6.59558	14.40	0.1370
3.25	38.66	5.80959	21.00	0.1930
3.5	42.34	6.21954	24.30	0.2130
3.75	45.35	5.39809	26.20	0.2110
4.01	49.93	5.39937	21.40	0.1810
4.5	50.13	4.8104	29.00	0.1690
4.77	50.84	5.0082	26.80	0.2030
5.24	52.89	4.80144	26.10	0.1560
5.5	53.22	4.02529	29.70	0.2100
6.03	55.37	3.81847	38.00	0.2090
6.25	55.49	3.59864	32.00	0.1510
6.49	55.83	3.81474	31.90	0.1550
6.74	55.91	3.79895	46.20	0.1860
7	56.12	3.79901	50.50	0.2500
7.75	54.79	4.20009	40.00	0.2127
8.5	54.3	4.40173	46.30	0.2630
9.05	54.8	4.40118	43.40	0.2490
9.51	53.73	3.79375	41.00	0.2150
10	51.71	5.39482	45.30	0.3280
10.45	47.23	6.1963	37.10	0.3070

vide the best pH stability throughout the experiment. The excess heat capacities vary significantly with pH (Table 1). At pH 3.0 a value of 14 kcal/mol ±8 kcal/mol was obtained, and at the pH optimum for cutinase (pH 8.5), these values rose to about 46 kcal/mol ± kcal/mol. As seen in Table 1 T_m displays a broad maximum in the range between pH 6.0 and 9.0. Original scans of cutinase at a scanrate of 90°C/h are given in Figure 1. The pH at which cutinase reveals its highest enzymatic activity (8.5) towards tributyrin [11], coincides with high thermal stability. Outside this pH range, T_m is shifting towards lower temperatures.

The thermograms also revealed that cutinase showed irreversible unfolding beyond pH 6.0. In the acidic region between pH 3.0 to pH 6.0 a denaturation peak has been detected upon reheating. At pH 4.0 the refolding capability of cutinase has been investigated and resulted in an 80% refolding of the native structure (Figure 2). The time necessary to regain 80% of the native protein was 3 hours at 5 degrees. Whereas in the basic region the refolding pathway seems to be blocked, since no transition can be detected upon reheating.

The influence of the scanrate on the apparent T_m at pH 4.0, 6.0, and 8.5 was also investigated (Figure 3). As is seen from Figure 3, the higher the scanrate, the higher the apparent T_m. However, the shift of T_m observed over the scanrates applied in the present study (10°C/h to 90°C/h) varied from 3°C at pH 8.5 to about 1°C at pH 6.0. When plotting the peak half width ($T_{1/2}$) of the calorimetric transitions observed against pH (Figure 4) a minimum is displayed at around pH 6.0 where the
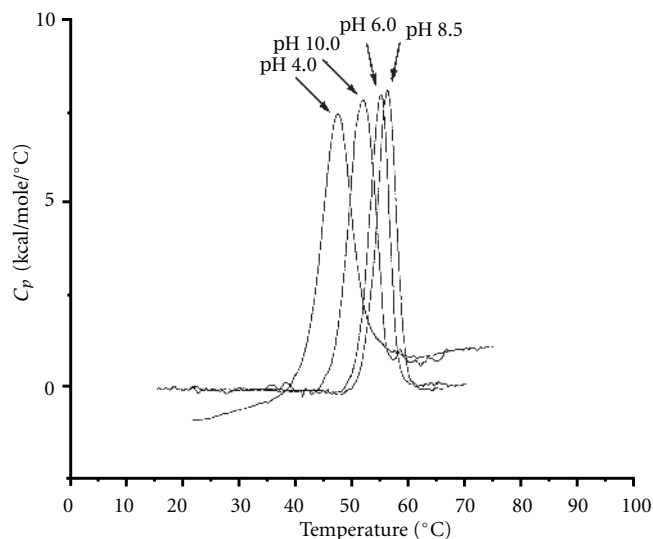
FIGURE 1: Original DSC scans of native cutinase at different pH values. The protein concentrations were 0.7 mg/ml for all experiments. The thermograms were all baseline corrected. The buffers were chosen as described in materials and methods.
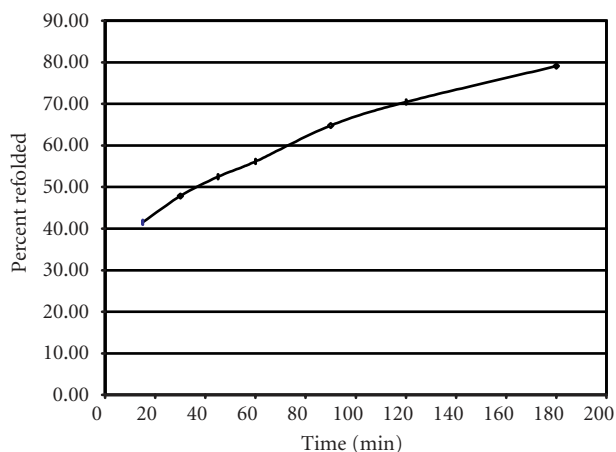

FIGURE 2: Reversibility of cutinase at pH 4.0. Cutinase has been heated and after cooling to 5 degrees different wait times have been introduced to account for the time necessary to refold the enzyme, before reheating the protein solution. The % refolding values have been obtained as relative values based on the values obtained from the first scan.

least variation in scanrate dependence has been observed.

The influence of pH on the titration state of the titratable residues of cutinase was investigated using TITRA [12, 13]. TITRA is based on the modified Tanford Kirkwood model and the Tanford Roxby iterative model for the calculation of the apparent pK_a values of solvent accessible residues. It also takes the ionic strength of the solution into account. We mapped the Delphi grid, as described in Materials and
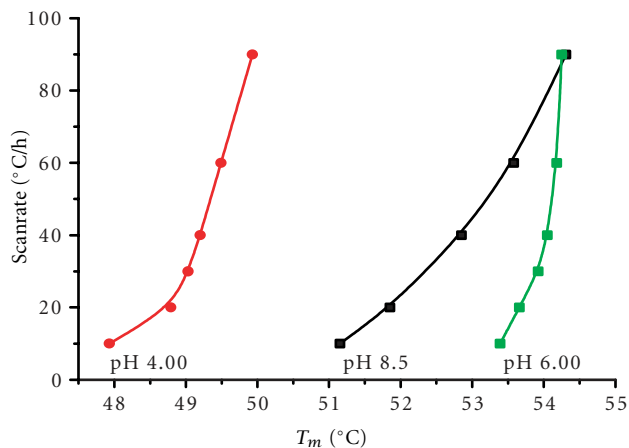

FIGURE 3: Scanrate dependence of T_m at different pH values. Scanrate dependence of cutinase at pH 4.00, 6.00, and 8.5. The scans were performed in three different buffers. The scanrates varied from 90 to 10°C/h. From the dependence of T_m on the scanrate the rate constant for the unfolding can be determined.
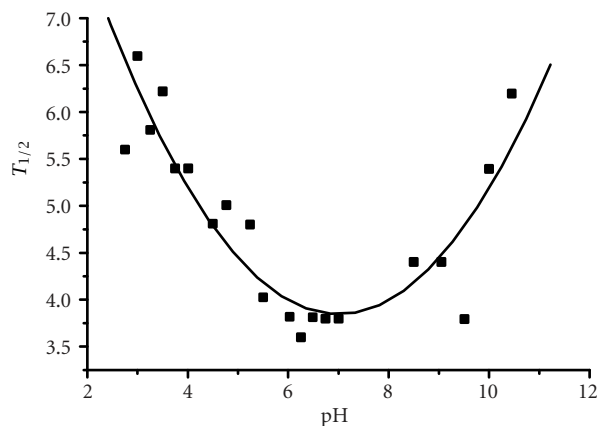

FIGURE 4: Peak halfwidth of cutinase over the observed pH range.

Methods on the surface of cutinase at pH 4.0, 6.0, 8.5, and 10.0 (Figure 6). Along the surface of the molecule a network of hydrogen bonds and also salt bridges (Figure 7), provides a possible explanation for the rise of T_m found around pH 6.0.

DISCUSSION

The thermal stability of cutinase versus pH displays the classical bell shaped appearance. Whereas the maximum stability is found in the pH range from 6–8.5, it decays rapidly at both flanking pH ranges (Table 1). It is interesting to note that pI for cutinase is 7.8, thus maximum stability is achieved close to the pI of the enzyme. Similar observations have been made for other enzymes [18]. In the acidic region cutinase displays
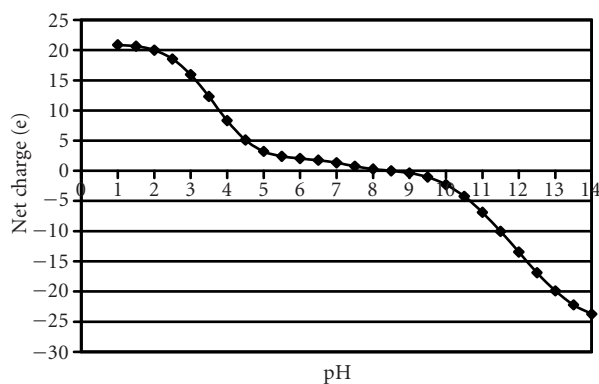
FIGURE 5: Titration curve of cutinase predicted by TITRA Plot of net charge of cutinase versus pH, calculated at a step width of 0.5 pH units.
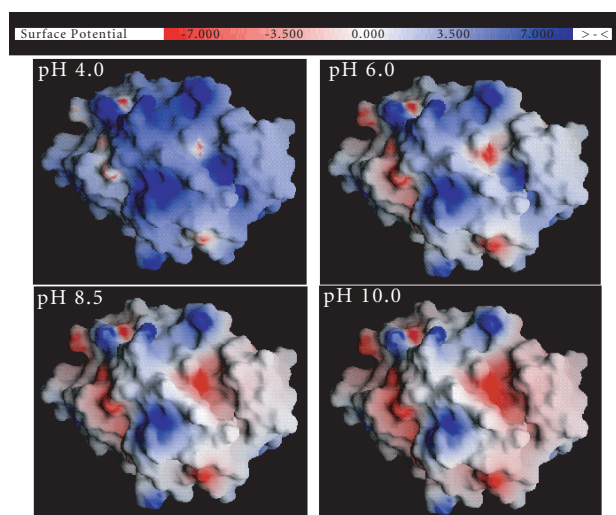

FIGURE 6: Visualization of the electrostatic potential on the surface at 4 different pH values of cutinase. Mapping the calculated partial charges to the surface of cutinase. Each titratable residue was predicted by TITRA. The potential distribution on the cutinase surface was calculated by DelPhi and displayed by Grasp. Charge at the surface of the enzyme at pH 4.0, pH 6.0, pH 8.5, and pH 10.0.
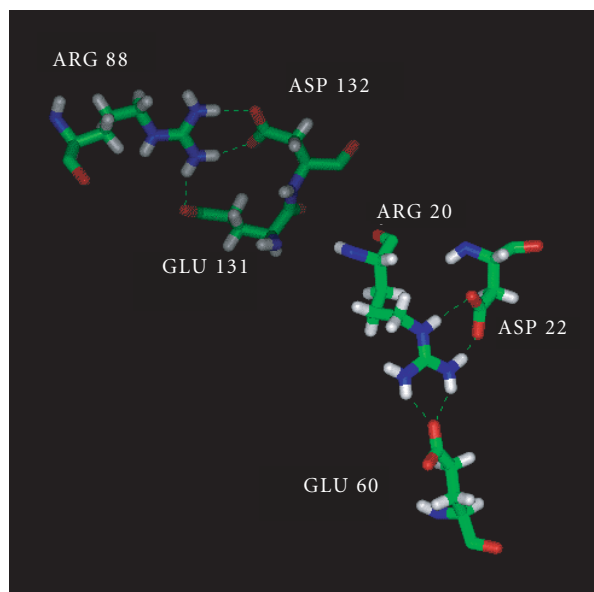

FIGURE 7: Salt bridges on the surface of cutinase. Amino acids involved in the formation of salt bridges on the surface of cutinase, as predicted by the pK_a shifts using the program TITRA.

a capability of refolding at temperatures below T_m (Figure 2). In the basic range, the thermograms appear irreversible.

At pH values different from pI, the net charge may lead to an electrostatic destabilization of the protein. A network of salt bridges has been identified on the surface of cutinase, based on the titration state behaviour as calculated by TITRA (Figure 7). Obviously pH will have an influence on the stabilising effect of such salt bridges, *e.g.*, if pH drops below the pK_a's for both ASP and GLU, the network will cease to exist. One can speculate if destabilising such networks could lead to less cooperative thermal transitions. The experimental observations of a broader transition peak seem to support this view. The calculated $\triangle H_{cal}$ and $\triangle H_{vH}$ bear a strong evidence for a non-two state behaviour, *i.e.*, the system is not an equilibrium system. A detailed molecular interpretation is outside the scope of the present paper, but it is relevant

to point out that most larger proteins share this feature with cutinase. Post denaturation self aggregates formed readily as seen by DLS at pH 8.5. Fluorescence studies revealed that the ability to aggregate can be reduced by lowering the concentration and changing pH (data not shown). The T_m's observed in the thermal studies displayed a strong dependence of the applied scanrate. This undoubtedly implies that the effective unfolding rate for cutinase is slow enough to be influenced by the scanrate.

The complex unfolding behaviour of cutinase may be linked with an ability of the structural framework of cutinase to adapt to the presence of a substrate. For other interfacially activated triglyceride lipases, it has been implied that the onset of enzymatic activity is coupled with a structural reorganisation, where the "lid" covering the active site is being moved aside [19]. Cutinase does not show such an interfacial activation, and does not possess a "lid" like structure, but it displays activity towards the same type of substrates as the other triglyceride lipases, although it has its highest activity towards short chain triglycerides. From X-ray crystallography the structure of cutinase has been solved although the first 16 aminoacids are disordered. It is still unclear where these aminoacids are located and which role they play in the structure of cutinase. Mass spectrometry (data not shown) reveals that our mature cutinase contains these 16 amino acids at the N-terminal end. If fully extended 16 Å can span a distance of more then 70 Å, thus any surface location on the 23 Å radius cutinase can be reached by this peptide fragment. This fragment appears to possess functional properties as it interferes with substrate specificity as revealed by an ongoing directed molecular evolution project (to be published). We propose that although cutinase does not have any X-ray visible structural feature similar to a "lid," it can access one or

more alternative conformational states when in contact with substrate and substrate aggregates, possibly utilizing the disordered first 16 amino acids. The same 16 amino acids may as well be involved in the onset of self-aggregation as indicated by the extreme $\triangle H_{cal}/\triangle H_{vH}$ ratios reported here (Table 1). H/D exchange and high resolution NMR could be employed to investigate this possibility in more details and maybe also clarify the role of the first 16 aminoacids.

The different apparent onset of enzymatic activity compared to the thermal stability profile as a function of pH can be explained by the different titration states of the active site residues (Figure 5). The formation of an active enzyme includes the correct formation of a hydrogen bond network in and around the active site, not only involving the residues of the catalytic triad, but also Tyr119, neighbouring the active site Ser120. This Tyrosine residue forms with its hydroxyl group a hydrogen bond with the backbone oxygen of the catalytic His188. The titration state of the catalytic triad (SER120, HIS188, and ASP175) is responsible for the hydrogen bonding among these three residues and for the level of enzymatic activity. The core residue in the triad is HIS188. The hydrogen network in the catalytic triad is established when HIS188 becomes deprotonated. Histidines usually display pK values between pH 6 to 7. The electrostatic potential of the active site environment is shown as a GRASP figure (Figure 6). At the pH with highest enzymatic activity the surrounding of the active site shows a slight negative electrostatic potential. This negative potential is achieved mainly due to the deprotonation of ASP175, GLU44 and deprotonation of the catalytic His188. Furthermore, the active site surrounding is populated with a set of tyrosine residues, contributing to the overall negative electrostatic potential at basic pH values. The lower T_m observed below pH 4.0 is likely due to the predominance of repulsive electrostatic forces, since at very acidic pH values the protein carries an excess of positive charge (see potential distribution at pH 4.0). This excess positive charge might also prevent the unfavourable hydrophobic interactions leading to irreversible aggregation in the neutral to basic pH region. This excess of positive charge will only be compensated for after deprotonation of Aspartic and Glutamic acid residues (pK$_a$ approx. 4–4.5). This coincides also with the rise in T_m values of cutinase after pH 4.5. The predicted pK values for E and D are close to the initial values for these amino acids, with the exception for D22 (pK 2.72) and E60 (pK 2.95), which are found to form a salt bridge with R20 (pK 12.94) and E131 (pK 3.72) and D132 (pK 3.14) are linked in another saltbridge with R88 (pK 12.98) on the surface of cutinase (Figure 7). This explains also their drastically shifted pK values. At maximum enzymatic activity (around pH 8.5) Aspartic and Glutamic acid residues are negatively charged, His188 of the catalytic triad is most likely neutral, tyrosine residues are predominantly protonated and Lysine and Arginine are positively charged. The electrostatic potential surrounding the active site is slightly negative (Figure 6). After pH 9–10 a drop in both T_m and catalytic activity is observed. This coincides with the titration of Tyrosine residues (pK values predicted by TITRA between 9.8–12.4, at pH 8.5). The excess of negative electrostatic potential in the active site due to deprotonation of Tyrosine residues can be seen in Figure 6. The Tyrosine residues and here especially Tyr119, once deprotonated loose their capability of donating hydrogens to hydrogen bonds and at the same time add to the molecule surface an excess of negative charge that is likely to destabilize the 3D structure of cutinase. This excess of negative charge in the active site and close to the catalytic triad may lead to a considerable structural destabilisation of the catalytic triad, since it is also in close proximity to the catalytic ASP175. The strong repulsion forces lead to a dramatic decrease not only in enzymatic activity, but also leads to a thermal destabilisation. This is in agreement with lower enzymatic activity as well as lowered thermal stability at very basic pH values.

For the enzymatic activity maximum found for cutinase at pH 8.5, the negative electrostatic potential inside and the surrounding of the active site, might as well be closely linked to the efficient catalysis. The substrate itself (triglycerides) are *per se* not carrying a charge, thus repulsion forces in substrate binding are not observed. But for the reaction products—a free fatty acid and a diglyceride, this is no longer the case. The free fatty acid generated in this process will most likely carry a negatively charged group, which will be strongly repulsed from the active site of the protein, leading to an efficient removal of the free fatty acid from the active site environment. This free fatty acid will be shot out of the active site like a rock from a catapult [20]. The negative charge in the active site cleft will provide this repulsion force for the product. At more acidic pH values, where the active site is not populated with a negative charge, the free fatty acid will actually be attracted to the active site and block it for further reactions rendering the enzyme inaccessible for another substrate molecule and the product itself will act as an inhibitor. This population of negative charges in the active site is found for all lipases and esterases and coinincides with their highest enzymatic activity [20].

Comparing the theoretical titration curve for cutinase (Figure 5) with the temperature profile and the peak half width plot (Figure 4), a pI slightly higher than the experimentally found pI for the enzyme pI = 7.8 is observed [21]. In the acidic region, where cutinase displays also a lower thermostability, a steep slope in the titration curve is found, corresponding to the titration of Aspartic and Glutamic acids residues, whereas in the range between pH 6–8, where cutinase is most thermostable and displays the minimum peak half width also, a very flat slope is observed, because the only residue being titrated is Histidine. Beyond pH 9.0 the steep slope correlates with the titration region of Tyrosines and later lysines. The thermostability starts to drop again, and also the peak half width starts to broaden, because of excess electrostatic charge on the surface of the enzyme. In Figure 6, the potential on the surface of cutinase is displayed. At pH 4.0 the enzyme is predominantly positively charged. At pH 6.0 the active site starts becoming slightly negative and at pH 8.5 it apparently displays an optimal electrostatic potential, whereas at pH 10.0 it shows an extreme negative potential. These electrostatic calculations of the surface of cutinase match well with the

observations from the DSC experiments and can explain also the influence of electrostatics on enzyme stability. The absolute difference between the excess positive charge and the excess negative charge found in cutinase may also be an explanation for the refolding capability of the enzyme at acidic pH values, whereas itself aggregates at basic pH values.

Molecular modeling and electrostatic calculations on the protein surfaces are powerful tools to explain experimental data in the case of cutinase, we could clearly see an effect between the activity, thermostability and underlying protein electrostatics. This model can be expanded to other proteins of this group as well. But can also be used for the investigation of other proteins which show irreversible denaturation in DSC experiments. The protein size influences the thermal unfolding behaviour of proteins, but also the electrostatics on the surface of the protein has a significant effect not only on the thermostability but also on the unfolding behaviour of the protein. We believe that the programs and methods used in this study are widely applicable to other proteins showing irreversible unfolding behaviour.

CONCLUSION

The data presented here provide a new insight of the thermodynamic behaviour of the single domain protein cutinase, and its stability and unfolding as a function of pH. The delayed onset of the enzymatic activity compared to the broad maximum of thermal stability can be explained by electrostatic effects around the active site of cutinase. According to our observations the pathway for unfolding clearly does not follow the two-state kinetic model. The reversibility of the thermograms seen at acidic pH values can also be explained by protein surface electrostatics. The irreversibility of the thermograms in the pH range above pI could not be linked by experimental techniques to self-aggregation phenomena, but strong evidence for this non-two state behaviour of unfolding is indicated by the large deviation from 1, seen in the $\triangle H_{\text{cal}} / \triangle H_{\text{v}}$ ratios.
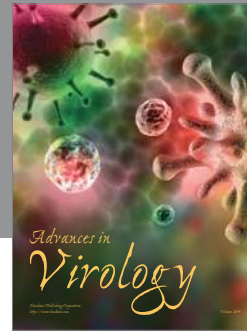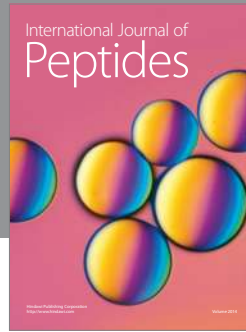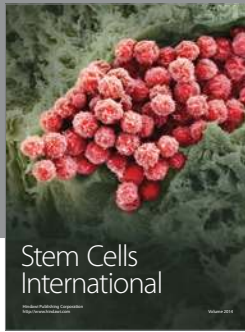
ACKNOWLEDGEMENTS

REFERENCES

[1] Garcia-Lepe R, Nuero OM, Reyes F, Santamaria F. Lipases in autolysed cultures of filamentous fungi. *Lett Appl Microbiol*. 1997;25(2):127–130.

[2] Crowhurst RN, Binnie SJ, Bowen JK, *et al*. Effect of disruption of a cutinase gene (cutA) on virulence and tissue specificity of *Fusarium solani f. sp*. Cucurbitae race 2 toward *Cucurbita maxima* and *C. moschata. Mol Plant Microbe Interact*. 1997;10(3):355–368.

[3] Ohnishi, *et al*. Genome structure and nucleotide sequence of a lipolyitc enzyme gene of *Aspergillus oryzae. FEMS Microbiol Lett*. 1995;15(126(2)):145–150.

[4] Taddei N, Chiti F, Paoli P, *et al*. Thermodynamics and kinetics of folding of common-type acylphosphatase: comparison to the highly homologous muscle isoenzyme. *Biochemistry*. 1999;38(7):2135–2142.

[5] Martinez C, De Geus P, Lauwereys M, Matthyssens G, Cambillau C. *Fusarium solani* cutinase is a lipolytic enzyme with a catalytic serine accessible to solvent. *Nature*. 1992;356(6370):615–618.

[6] Sanchez-Ruis JM. Theoretical analysis of Lumry-Eyring models in differential scanning calorimetry. *Biophys J*. 1992;61:921–935.

[7] Freire E, van Osdol WW, Mayorga OL, Sanchez-Ruis JM. Calorimetrically determined dynamics of complex unfolding transitions in proteins. *Annu Rev Biophys Chem*. 1990;19:159–188.

[8] Loladze VV, Ibarra-Molero B, Sanchez-Ruiz JM, Makhatadze GI. Engineering a thermostable protein *via* optimization of charge-charge interactions on the protein surface. *Biochemistry*. 1999;38(50):16419–16423.

[9] Jaenicke R, Zavodszky P. Proteins under extreme physical conditions. *FEBS Lett*. 1990;268(2):344–349.

[10] Sambrook J, Fritsch EF, Maniatis T. Molecular Cloning: A Laboratory Manual. 2nd ed. Cold Spring Harbor, NY: Cold Spring Harbor Laboratory Press; 1989.

[11] Lauwereys M, De Geus P, De Meutter J, Stanssens P, Matthyssens G. Cloning, Expression and Characterization of Cutinase, a Funagl Lipolytic Enzyme. In: Chemie V, ed. Lipases: Structure, Mechanism and Genetic Engineering. Vol 16; 1990:243–251.

[12] Martel P, Baptista A, Petersen SB. Protein Electrostatics. El Gewely MR, ed. Biotechnology Annual Reviews. 1996:315–372.

[13] Petersen MT, Martel P, Petersen EI, Drablos F, Petersen SB. Surface and electrostatics of cutinases. *Methods Enzymol*. 1997;284:130–154.

[14] Tanford C, Kirkwood JG. Theory of protein titration curves, I: general equations for impenetrable spheres. *J Am Chem Soc*. 1957;79(20):5333–5339.

[15] Tanford C, Roxby R. The interpretation of protein titration curves: application to lysozyme. *Biochemistry*. 1972;11(11):2192–2198.

[16] Nicholls A, Sharp K, Honig B. Structure, function and genetics. *Proteins*. 1991;11(4):281ff.

[17] Ibarra-Molero B, Loladze VV, Makhatadze GI, Sanchez-Ruiz JM. Thermal versus guanidine-induced unfolding of ubiquitin: an analysis in terms of the contributions from charge-charge interactions to protein stability. *Biochemistry*. 1999;38(25):8138–8149.

[18] Relkin P. Thermal unfolding of β-lactoglobulin, α-lactalbumin, and bovine serum albumin: a thermodynamic approach. *Int J Food Sci Nutr*. 1996;36(6):556–601.

[19] Winkler FK, D'arcy A, Hunziker W. Structure of human pancreatic lipase. *Nature*. 1990;343:771–774.

[20] Petersen MTN, Fojan P, Petersen SB. How do lipases and esterases work: the electrostatic contribution. *J Biotechnol*. 2001;85:115–147.

[21] Mannesse ML, Boots JW, Dijkman R, *et al.* Phosphonate analogues of triacylglycerols are potent inhibitors of lipase. *Biochim Biophys Acta*. 1995;1259(1):56–64.

* Corresponding author.
E-mail: sp@bio.auc.dk
Fax: +45 98141808; Tel: +45 96358469